Title

Neural responses to implicit forms of peer influence in young adults

Journal

Social Neuroscience, 16(3)

ISSN

1747-0919

Authors

Venticinque, Joseph S
Chahal, Rajpreet
Beard, Sarah J
et al.

Publication Date

2021-05-04

DOI

10.1080/17470919.2021.1911843

Peer reviewed

HHS Public Access

Author manuscript

Soc Neurosci. Author manuscript; available in PMC 2022 June 01.

Published in final edited form as:

Soc Neurosci. 2021 June ; 16(3): 327–340. doi:10.1080/17470919.2021.1911843.

Neural Responses to Implicit Forms of Peer Influence in Young Adults

Joseph S. Venticinque, B.A.[1,2], **Rajpreet Chahal, Ph.D.**[3], **Sarah J. Beard, M.S.**[1,2], **Roberta A. Schriber, Ph.D.**[1,2], **Paul D. Hastings, Ph.D.**[2,4], **Amanda E. Guyer, Ph.D.**[1,2]

[1]Department of Human Ecology, University of California, Davis, Davis CA, USA;

[2]Center for Mind and Brain, University of California, Davis, Davis, CA, USA;

[3]Department of Psychology, Stanford University, Stanford, CA, USA;

[4]Department of Psychology, University of California, Davis, Davis, CA, USA

Abstract

Young adults are acutely sensitive to peer influences. Differences have been found in neural sensitivity to *explicit* peer influences, such as seeing peer ratings on social media. The present study aimed to identify patterns of neural sensitivity to *implicit* peer influences, which involve more subtle cues that shape preferences and behaviors. Participants were 43 young adults (M_{Age} = 19.2 years; 24 males) who underwent functional magnetic resonance imaging while completing a task used to assess neural responses to implicitly "socially tagged" symbols (previously judged by peers as liked vs. not liked, thus differing in apparent popularity) vs. novel symbols that carried no social meaning (not judged by peers). Results indicated greater activity in brain regions involved in salience detection (e.g., anterior cingulate cortex) and reward processing (e.g., caudate) to socially tagged vs. novel symbols, and particularly to unpopular symbols. Greater self-reported susceptibility to peer influence was related to more activity in the insula and caudate when viewing socially tagged vs. novel symbols. These results suggest that the brain is sensitive to even subtle cues varying in level of peer endorsement and neural sensitivity differed by the tendency to conform to peers' behaviors particularly in regions implicated in social motivation.

Keywords

social influence; young adulthood; fMRI; peers; popularity

Susceptibility to peer influence is the process by which peers directly or indirectly influence one's thoughts, feelings, and behaviors (Turner, 1991). Peers, especially relative to parents, normatively gain more sway across the second decade of life (Nelson et al., 2016), as youths navigate increasingly complex social situations and continue to form their identities (Brown, 2004; McLean, 2005). Although peer influence has long been thought to peak in mid-adolescence (Brown, 1990), Steinberg and Monahan (2007) have found that self-reported susceptibility to peer influence linearly increases throughout middle adolescence, peaking in

Corresponding author: Joseph S. Venticinque, Center for Mind and Brain, Department of Human Ecology, University of California Davis, 267 Cousteau Place, Davis, CA 95618, jventicinque@ucdavis.edu, Phone: (530)-754-4545.

young adulthood around 18 years of age. Another index of peer susceptibility is the brain's response to peer-evaluated social information. Little is known, however, about individual differences in these neural responses, particularly to implicit forms of influence that involve processing subtle social cues. Demonstrating the brain's sensitivity to subtle cues may help expand understanding of social media use and consumer behavior as well as inform actionable content for programs and interventions designed to leverage the power of peer influence. Thus, the goal of the present study was to investigate neural responses to implicit peer influence alongside self-reported differences in peer susceptibility in young adults.

Elevated susceptibility to social influence observed in late adolescence and young adulthood may reflect heightened sensitivity of brain regions involved in social cognition and reward processing during this period. For example, among late adolescents, the medial prefrontal cortex (mPFC) and temporoparietal junction, regions implicated in mentalizing, have shown greater activity when participants viewed images rated as more vs. less liked by peers (Welborn et al., 2015). Similarly, participants showed greater activity in the mPFC when they observed peers' performance during a public goods donation game compared to trials without peer observation (van Hoorn et al., 2016a). Additionally, Sherman and colleagues (2016) found greater activity in the nucleus accumbens (NAcc), a hub of the brain's reward-processing network, when adolescents viewed social media photographs understood to be popular among peers through explicit displays of "likes" relative to less popular photographs. In a second study, college-aged participants showed even greater NAcc responsivity to popular social media photos than did younger adolescents (Sherman et al., 2018), suggesting that neural reward sensitivity to peer influence remains elevated in young adulthood.

Not all individuals are equally susceptible to peer influence, an issue that is important to investigate because this variability may be linked to positive or negative behavioral and health outcomes. Indeed, greater self-reported susceptibility to peer influence has been associated with engaging in higher rates of behaviors that can put health at risk (Dahl, 2011; Mirman & Curry, 2016; Monahan et al., 2009) or promote well-being (Wentzel & Meunks, 2016; Choukas-Bradley et al., 2015; van Hoorn et al., 2016b). Furthermore, one neuroscience perspective highlights the brain as another important source of individual differences in social susceptibility, proposing that the variability in features (e.g., structure, function) of certain neural regions/circuitry modulate the effects of social contexts on both positive and negative outcomes (Schriber & Guyer, 2016). Yet, prior to applying this framework to outcomes, more research is needed to determine what brain regions respond to different types of peer influence in order to demonstrate who is more or less susceptible to peer influences. Additionally, neural responses measured alongside paper-and-pencil measures of peer susceptibility are needed to understand how such peer susceptibility manifests in quantifiable ways across different levels of analysis.

Much of the current neuroimaging work examining peer influence focuses on explicit influences, such as delivering overt displays of valenced evaluations from peers. Several studies have used simulated feedback designs in functional magnetic resonance imaging (fMRI) paradigms to deliver positive and negative evaluation to participants from hypothetical peers (Guyer et al., 2009; Guyer et al., 2012; Somerville et al., 2006; Jarcho et

al., 2016). Similar studies have used a simulated social media platform to deliver explicit displays of peer ratings of photographs (e.g., “50 likes”; Sherman et al., 2016). However, peer influence also occurs in more *implicit* forms, as social information is embedded subtly in everyday contexts. For example, logos of popular brands can be salient social status symbols that hold indirect value deemed by peers’ opinions. Little is known, however, about how these implicitly conveyed markers of peer opinion, and thus potential social standing, are processed by the brain and relate to behavior. Additionally, a limitation of existing neuroimaging research is that many fMRI paradigms use relatively obvious manipulations of peer influence. For example, participants often view peer judgments while anticipating that they will provide their own judgments, either conforming or not conforming to peer opinions. Thus, sensitivity to peer influence may be captured more fully through implicit, *incidental* exposures to social cues.

In one of the few studies to investigate neural correlates of implicit peer influence, Mason and colleagues (2009) examined neural responses to socially tagged symbols in a sample of 12 adult men. Participants were presented with pairs of abstract symbols supposedly rated by peers in terms of how much the peers liked the symbols. For each trial, a picture of a peer was presented and a box highlighted which of the two symbols the peer preferred. As such, symbols were implicitly “socially tagged” and instantiated to be either popular (selected in 90% of trials) or unpopular (selected in 10% of trials). Subsequently, a subset of these socially tagged symbols, along with novel symbols not previously shown, were presented to participants during a fMRI scan. Notably, unlike previous studies in which participants were told explicitly about how much others liked the stimulus (Sherman et al., 2016), information about popularity was instantiated through implicit repeated exposures to peer preferences (Mason et al., 2009). Due to the novel design of the study, the authors first sought to broadly establish whether or not participants would be neurally sensitive to stimuli that were instantiated through this more implicit approach (i.e. socially tagged vs. novel symbols). Next, to further disentangle the effects of valence, the authors tested differences in neural response to popular vs. unpopular information. Results indicated that participants exhibited greater neural sensitivity in brain regions related to salience detection and mentalizing (e.g., mPFC) to socially tagged vs. novel symbols. Furthermore, participants displayed greater neural responses in the caudate nucleus, a region involved in reward processing, to popular versus unpopular symbols. These results suggest that the brain is quite sensitive to peer-evaluated information and detects subtle differences in peer-conferred valence. This formulation aligns with other findings showing that adults exhibit greater neural activity in the mPFC to popular versus unpopular organic food brands (Fehse, 2017), given that a brand’s ‘popularity’ is established by other consumers’ aggregated buying preferences.

The present study aimed to expand understanding of the neural processes involved in implicit instantiations of peer influence via information that varied in peer preference and the extent to which neural responses related to self-reported susceptibility to peer influence. Additionally, the current study sought to address calls to move the field beyond reliance on findings from WEIRD populations (Henrich et al., 2010; Legare & Harris, 2016), by drawing on a sample of Mexican-origin young adults from families of low to moderate income. Using an extension of Mason et al.’s (2009) paradigm, the current study tested three hypotheses. First, brain regions involved in salience detection (e.g., mPFC, ACC) would

show increased neural activity to socially tagged vs. novel symbols. Second, through repeated exposures to peer evaluation that instantiated degree of popularity, reward-related brain regions would show increased activity to popular vs. unpopular symbols. Finally, activity in salience-detecting and reward-processing regions in response to implicit social information would be related to self-reported susceptibility to peer influence; however, formal predictions of directionality were not made given the nascent literature.

Method

Participants

Participants were 46 young adults from Mexican-origin families (24 males, M_{Age} = 19.2 years, SD = .54, range = 18.3–20.1 years, 74.4% born in the United States) who had previously been participating in a neuroimaging sub-study of a prospective, 10-year, longitudinal study on risk and protective factors of substance use in Mexican-origin youth. Participants in the parent study included 674 Mexican-origin families (variously first-, second-, and third-generation) who had a fifth-grade child (51.2% male, M_{Age} = 10.4 years, SD = .61) that was drawn randomly from school rosters in Sacramento and Woodland, California, during the 2006–2007 and 2007–2008 school years. For the neuroimaging sub-study, 90 participants from the parent study were recruited based on data from measures (Elliot et al., 1985; Shaffer et al., 2000; Gibbons et al., 2004) indicating they had either abstained from and would continue to do so (N = 47) or engaged in (N = 43) substance use as of the 9th grade (age 14–15). Three years later, a smaller neuroimaging sub-study was launched, for which these participants were contacted again and invited to participate. Of the 90 participants, 46 enrolled (25 of whom had engaged in substance use as of the 9th grade) and completed the Social Influence Task as well other tasks in this neuroimaging session. Three participants were excluded from analyses due to excessive motion in the scanner, yielding a sample of 43 young adults for all analyses.

Procedures

Study procedures were approved by the university's Institutional Review Board. Participants visited a medical research facility to participate in the neuroimaging component of the study. Procedures during the visit included: obtaining participants' written informed consent, training on fMRI tasks using a mock scanner, completing questionnaires, and undergoing a structural MRI and three-tasked based fMRI scans (totaling about 1.5 hours), one of which was the social influence task (SIT) examined in the present study. All participants elected to complete all measures in English. Participants were monetarily compensated for study participation.

Measures

Resistance to peer influence—The Resistance to Peer Influence scale (RPI; Steinberg, & Monahan, 2007) was collected the same day as the scan to measure self-reported resistance to the attitudes and behaviors of peers. The RPI consists of 10 different scenarios with dichotomous, conflicting statements regarding peer influence (e.g., "Some people go along with their friends just to keep their friends happy" BUT "Other people refuse to go along with what their friends want to do, even though they know it will make their friends

happy"). Participants indicated which of the two opposing statements best described them, and for the selected statement, whether it was "sort of true" or "really true" for them, resulting in a four-point scale. Higher scores indicate greater resistance to peer influence (i.e., less peer susceptibility), whereas lower scores indicate less resistance to peer influence (i.e., greater peer susceptibility). Cronbach's alpha was .82 in the current study, suggesting good reliability.

Neural response to social influence—The Social Influence Task (SIT) was an adaptation of the task used by Mason, Dyer, and Norton (2009). The task included 30 abstract symbols that were unfamiliar and neutral, thus free from social meaning prior to participation in the study. Twenty of the 30 symbols were selected randomly to be used in the pre-scanning portion of the task: 10 to be implicitly tagged as "popular" and 10 implicitly tagged as "unpopular." The remaining 10 symbols were used as the novel symbols shown only during the fMRI scan. Two hundred same-aged peer faces were included in the pre-scan "social instantiation" part of the SIT.

Social instantiation task—For the pre-scan "social instantiation" part of the task, participants were told hundreds of same-aged individuals were shown pairs of abstract symbols and that these ostensible peers indicated which symbols they preferred. Participants were also told they would see pictures of these peers, followed by a display of the two symbols the peer saw and which symbol the peer selected. Participants then had to press one of two designated buttons in accordance with the symbol the peer preferred. Participants were told to pay close attention to which symbols were selected but that they would not be tested on this information.

Participants completed 200 trials (each 2500ms in duration) in which a randomly selected picture of a new same-aged actor appeared in the center of the screen (lasting 750ms). Next, two symbols appeared below the picture and a green box appeared around the symbol that was supposedly preferred by the peer (lasting 1250ms). Trials were separated by a 500ms fixation cross. Participants were instructed to make a left or right key press using arrow keys on the keyboard to indicate the side of the screen on which the chosen symbol was presented. For half of the trials, the chosen symbol was displayed on the left and for the other half, on the right, to promote participant engagement. Symbols were implicitly socially tagged as popular vs. unpopular through the rate at which they were shown to be the preferred symbol; popular symbols were shown to be preferred in 90% of the trials in which they appeared as part of a symbol pairing, whereas unpopular symbols were preferred in only 10% of relevant trials. All symbols were shown the same number of times. The purpose of this pre-scan task was to incidentally expose participants to peers' preferences.

Scanning phase: Social Influence Task—For the part of the SIT that occurred in the scanner, participants were instructed that they would view symbols again, some of which they saw before and some of which were new. Participants completed a 1-back memory task in which they were told to press a button each time they saw the same symbol presented twice in a row. The purpose of the latter instruction was to ensure that participants paid attention to all symbols during the task.

The task was presented in two runs of approximately 8 minutes each. Each run contained 90 trials of fixed duration (750ms): 27 popular, 27 unpopular, and 36 novel symbols, with 6 trials from each category being a repeated-symbol trial. In the interval between stimuli, a fixation cross was shown for a variable duration of 2–10s (jittered period) to maximize general linear model contrast efficiency and reduce expectancy effects (Figure 1). Trial types were pseudo-randomized within each run and run order was counterbalanced across participants. Stimuli were presented using E-Prime 2.0 software (Psychology Software Tools, Pittsburgh, PA) and back projected onto a screen at the end of the bore of the magnet that participants viewed using a mirror mounted to the head coil. Foam padding was used around the participant's head to reduce motion.

Following the scan, participants rated how much they liked each symbol on a 7-point scale from 1 = "dislike a lot" to 7 = "like a lot" and indicated whether symbols presented during the instantiation period appeared to be more liked than others ("yes", "no", or "not sure"). This was to assess whether participants were able to consciously recall differences in implicit peer preferences. Mean ratings of each symbol type were tested for possible differences in participants' own reported liking of the symbols.

Image acquisition and data preprocessing

The scan was conducted on a Siemens 3-Tesla TIM Trio MRI scanner with a 32-channel head coil (Siemens Medical Solutions, Erlangen, Germany). Scanning parameters for the EPI T2-weighted functional image acquisition were voxel size=3.5 × 3.5 × 3.5mm, number of slices=35, slice thickness=3.5mm, repetition time (TR)=2000ms, echo time (TE)=27ms, flip angle=80°, interleaved slice geometry, field of view (FOV)=224mm. The first four volumes were discarded to ensure magnet stabilization. A high-resolution structural scan was acquired per subject using a T1-weighted standardized magnetization-prepared, spoiled gradient recalled echo sequence (208.95mm slices; TR=2500ms; TE=4.33ms; flip angle=7°; FOV=243mm, inversion time: 800ms, 256 × 256 matrix). Preprocessing and data analyses were conducted using Analysis of Functional NeuroImages (AFNI: www.afni.nimh.nih.gov/afni, version AFNI_18.2.14; Cox, 1996). Preprocessing of functional data included slice timing correction, rigid body motion correction with 6 degrees of freedom, co-registration of functional data with brain-extracted structural images normalized to the Montreal Neurological Institute (MNI) stereotaxic atlas, and nuisance regression of the 6 rigid body motion parameters. Proper alignment was confirmed visually for each participant. Spatial smoothing with 4-mm Gaussian kernel, full-width at half maximum was conducted. Given the relatively small sample and the small size of the anticipated regions of activation, we used this more minimal smoothing strategy to increase the signal-to-noise ratio and better specify structural sub-regions. Although the literature indicates a lack of consensus regarding the degree of smoothing to apply for various reasons (e.g., location and size of brain regions; Botvinik-Nezer et al., (2020)), this approach has been used in studies with similar sample sizes and acquisition parameters (Li et al., 2018; Xu et al., 2019), and recent reports indicate that modeling head motion may have more of an effect on results than explicit smoothing (Botvinik-Nezer et al., 2020). Volumes with head motion >1mm from the previous volumes were censored during further processing. Three participants missing >20%

of total volumes following motion censoring were excluded resulting in a total sample of 43 participants for analyses, as mentioned above.

fMRI data analysis

First level processing—For first level processing, the SIT was modeled as an event-related design with 6 trial types (popular, unpopular, novel, and repeat symbols, button presses, and fixation). Using AFNI's *3dDeconvolve* function, each trial type was modeled as a gamma variant function and blood-oxygen-level dependent (BOLD) responses were obtained for each participant. In line with Mason et al. (2009), the contrasts of interest were "socially tagged" (popular + unpopular) symbols > novel symbols and popular > unpopular symbols. The 6 motion parameters were included in the model to account for variation due to head motion.

Second level processing—Second level processing was conducted using a whole-brain, voxel-based approach. Using AFNI's *3dttest++* function, group-level parameter estimates (β) and *t*-contrast images were computed for contrasts of "socially tagged vs. novel" and "popular vs. unpopular" symbols. As a physical measure of effect magnitude (as opposed to a dimensionless value, such as Cohen's *d*), percent signal change values are presented for all results and refer to the specific cluster peak of the given contrast (Chen et al., 2017). Additionally, main effects associated with differences in RPI scores for both contrasts of interest were assessed in the whole-brain, group-level analysis. For the whole-brain analyses of both contrasts (i.e., socially tagged vs. novel and popular vs. unpopular), scores on the RPI were included as a covariate of interest, whereas participant sex and substance use at original recruitment (yes/no substance use as of age 14) were included as nuisance variables. RPI scores were mean-centered prior to being entered into the model. The anatomical region of each cluster identified by the whole-brain analyses was labeled using AFNI's *WhereAmI* function based on being the closest region within 3mm of the peak of activation around which the cluster was centered. Using gray-white matter probability (*p*) maps included in *WhereAmI*, all reported clusters were demonstrated to be more likely to appear in gray vs. white matter. Multiple comparison correction was applied using cluster size and voxel significance information. AFNI's *3dclustim* program, which uses Monte Carlo simulations based on the average spatial autocorrelation parameters, was used to determine thresholding parameters. Autocorrelation parameters were estimated from subject-level residuals using AFNI's *3dFWHMx* tool (a = .83, b = 3.52, c = 8.99). This analysis revealed that for a 2-sided test using nearest neighbor clustering (voxels clustered together in which faces touch), at least 19 contiguous voxels initially thresholded at p=.005 were necessary to achieve cluster-level corrected alphas <.05.

Plotting and Visualization—Further analyses were conducted to decompose and plot interactions from activation clusters identified in the whole brain analyses. First, using AFNI's anatomical atlases, masks were created around significant clusters identified from the whole-brain analysis. Next, using *3dmaskave* and *3dROIstats*, beta coefficients were extracted from these regions based on the symbol types of comparison (e.g., popular vs. unpopular) to determine the unique signal associated with each type. A similar method was used to create masks around significant clusters identified in the whole-brain analysis that

differed based on scores on the RPI. Beta coefficients of relevant contrasts were extracted from masks of these regions.

Results

Whole-brain task activation

To test hypothesis one, neural activation to socially tagged (popular and unpopular) symbols relative to novel symbols was compared. Two significant clusters whose peak was centered in the right ACC and right insula were found that exhibited greater neural activity to socially tagged versus novel symbols (Table 1; Figure 2). Additionally, brain regions involved in perceptual (e.g., occipital lobe, fusiform gyrus) and somatosensory processing (e.g., precentral gyrus) displayed greater activation when viewing socially tagged versus novel symbols (Table 1).

To test hypothesis two, neural activation to viewing popular relative to unpopular symbols was compared. Two significant clusters, whose peak was centered in the left caudate and left middle cingulate, exhibited greater neural activity when viewing popular relative to unpopular symbols (Table 2; Figure 3). Contrary to our hypothesis, participants displayed greater *de*activation to popular versus unpopular symbols in these two regions, which are implicated in reward processing and salience detection, respectively. To depict these results, extracted beta values for popular and unpopular symbols are presented for these clusters with higher values being associated in response to unpopular symbols in both the left caudate ($\beta = .04$) and the left middle cingulate ($\beta = .02$). Furthermore, brain regions implicated in memory (e.g., hippocampus, middle temporal gyrus) and integration of visual information (e.g., inferior temporal gyrus) exhibited greater activation to popular relative to unpopular symbols (Table 2).

The third hypothesis tested whether neural activation to socially tagged vs. novel symbols related to mean-centered RPI scores. For clarity of interpretation, RPI scores were reversed before being entered into the model (i.e., higher scores reflected greater susceptibility to peer influence). Significant clusters were identified in the contrast between socially tagged and novel symbols in relation to RPI scores. Greater susceptibility to peer influence was associated with greater activation in the right insula and right caudate (Table 3; Figure 4), as well as regions involved in perceptual processing (e.g., occipital lobe, fusiform gyrus) and integration of visual information (e.g., inferior temporal gyrus) to socially tagged versus novel symbols (Table 3). In examining the valence of socially tagged symbols, greater susceptibility to peer influence was associated with greater activation in the left insula and right ACC to popular relative to unpopular symbols (Figure 5). Finally, greater susceptibility to peer influence was associated with greater activation in brain regions involved in somatosensory processing (e.g., supramarginal gyrus) and memory (e.g., hippocampus and precuneus) when viewing popular versus unpopular symbols. (Table 4).

Supplemental analyses were conducted to identify clusters of neural activation for each contrast (i.e., socially tagged > novel and popular > unpopular symbols) that differed by substance-use history at age 14 (i.e., “no use”, or “some use”). Results indicated that no regions implicated in salience detection or reward processing described in the current study

differed based on substance use history (Table S1 and S2). Additionally, a *t*-test was conducted testing differences in RPI scores between age 14 substance-use history recruitment groups, yielding non-significant results, $t(41) = -0.40$, $p = .68$.

Attention and manipulation checks

To assess participant attention during the task, we calculated overall accuracy on button presses during the 36 "repeat" trials ($M = 86.1\%$, $SD = 2.2$). In order to better characterize incorrect responses due to indiscriminate button pushes, we computed a discrimination index (Pr; i.e., hit rate – false alarm rate). Results of this analysis revealed an average discrimination of 151 out of 180 trials ($M = 83.8\%$, $SD = 3.1$), suggesting that participants were reasonably engaged throughout the task.

For the post-scan survey, a repeated measures analysis of variance was conducted to compare participant ratings of how much they liked each of the "popular", "unpopular", and "novel" symbols post scan. There was no significant difference in scores between ratings of popular ($M = 4.40$, $SD = .85$), unpopular ($M = 4.43$, $SD = .82$) and novel ($M = 4.30$, $SD = .90$) symbols, $F(2, 42) = .79$, $p = .37$. In other words, participants did not differ in their own explicit preference ratings of the task symbols following the scan. Next, participants reported whether "some symbols appeared to be liked more than others" during the instantiation period: 4 (9.3%) reported "no", 36 (83.7%) "yes", and 3 (7.0%) "not sure", $X^2(2, N = 43) = 33.5$, $p < .001$, suggesting the instantiation was successful in assigning popularity values to certain symbols, and participants accurately recognized that some symbols appeared more liked than others. Finally, when participants were asked if they "remembered seeing any of the symbols in the fMRI task during the instantiation period," 21 (48.8%) reported "no", 9 (21.0%) "yes", and 13 (30.2%) "not sure", $X^2(2, N = 43) = 11.0$, $p = .01$, suggesting that many participants were unable to consciously recall if they were shown the same symbols in both portions of the task.

Discussion

Young adults vary in their susceptibility to being influenced by their peers, and having procedures to identify the neural activity corresponding with being more versus less likely to having one's judgments and decision-making influenced by the consensus of others is essential for advancing brain-based models of social susceptibility (Schriber & Guyer, 2016). The current study was designed to examine neural responses to symbols that were implicitly conveyed as popular or unpopular among peers, as well as to novel symbols carrying no social information. Partially consistent with previous research (Mason et al., 2009), our results showed that young adults are neurally sensitive to the presence and evaluative content of implicit information concerning peer preferences in brain regions involved in the detection of salience (e.g., right ACC, insula) and reward processing (e.g., caudate). This suggests that these regions are also sensitive to even *incidental* exposure to information that holds social value via peer opinions (e.g., logos of popular brands).

One explanation for the current findings pertaining to socially tagged information may be that young adults are simply motivated to align their own preferences to match those of their peers. Although few neuroimaging studies of social conformity exist, the present results

involving the ACC and insula are consistent with other studies that examined different domains of social influence. For example, greater ACC activation has been reported in response to experiences of social exclusion during a ball-tossing game (Eisenberger et al., 2003) and Stallen and Sanfey (2015) have suggested that the ACC may be similarly involved in conforming to peer norms, potentially as a method to avoid potential social exclusion. The current findings also implicated the insula in responding to peer-evaluated social information. Greater insula activation has been associated with the enforcement of social norms through threats of punishment during a financial transfer game (Spitzer et al., 2007), and during unfair offers during an ultimatum game (Sanfey et al., 2003) among young adults. Resting state functional connectivity analyses have provided evidence for an insula-ACC network that is likely involved in environmental monitoring and detection of emotional salience (Taylor et al., 2009).

The current study also found that young adults displayed lower levels of neural activation in brain regions implicated in salience detection and reward processing when viewing popular relative to unpopular social information. This finding contrasts with results reported by Mason and colleagues (2009), in which adults displayed greater right caudate responses to popular vs. unpopular symbols. Indeed, consistent with their work, an fMRI study of peer influences on music preferences (Berns et al., 2010) found that participants showed greater neural responses in caudate and ACC during exposure to music deemed popular, as opposed to unpopular, by peers. It has been suggested by these and other authors that attuning to popular material reflects the drive to be socially accepted. However, the divergent findings of the present study raise the possibility that tracking what is *disliked* by peers can also be instrumental to this goal. That is, avoiding behaviors or choices that are disliked by peers and likely to lead to social rejection may be more critical and involve more salient information than conforming to what peers like. For instance, if a brand of clothing is learned to be unpopular among friends, making sure to not wear it and to communicate disapproval of it can help preserve one's social status and belonging (Nelson & Guyer, 2011). On a methodological note, our findings may have differed from those of Mason and colleagues (2009) due to our increased ability to detect effects owing to a larger sample size.

Young adults with a higher self-reported susceptibility to peer influence demonstrated greater activity in the right insula, a region implicated in salience processing as well as various forms of empathy (Uddin et al., 2017) when viewing socially tagged relative to novel information. Thus, it appears that young adults who reported being more susceptible to pressure from peers may be more "tuned in" to implicit forms of peer-evaluated information. Similarly, higher peer susceptibility was related to greater neural engagement of the right caudate when viewing socially tagged information, suggesting that peer-sensitive young adults may pay increased attention to implicit peer information, but it also may be particularly rewarding to be aware of the preferences of others. Participants who reported greater susceptibility to peer influence displayed *greater* neural activity in the insula and ACC when viewing popular relative to unpopular information, which differs from the result that did not include self-reported peer susceptibility in the model. In other words, overall, young adults in this sample may have been more attentive to information about what peers disliked as opposed to liked. However, for those who reported higher susceptibility to influence from peers, popular symbols preferentially engaged salience detection and reward-

processing regions, suggesting a differential pattern for individuals who were more peer-sensitive.

Additional cognitive processes are engaged when exposed to peer-rated information, beyond detecting its salience and potential associated rewards. This is evidenced by our finding activity in brain regions not included in our hypotheses that are involved in visual (e.g., occipital lobe) and memory processing (e.g., hippocampus). Differences in neural activation in these regions may suggest that processing of implicit peer influence may be partly driven by one's familiarity with the stimulus. However, these concerns are mitigated by our results that indicated that the unpopular symbols, which were the symbols that were *not* outlined by a box in the instantiation phase, were the most salient, suggesting that participants were not simply reacting to those symbols to which most of their attention had been drawn. Thus, this suggests that neural processing of solely the familiarity of a stimulus may differ from also considering the peer-evaluation attached to it. To further disentangle peer preference from visual saliency and motoric response, future work could draw on a task design of blocked trials where selected symbols are outlined by a green box and non-selected symbols are outlined by a red box, and participants alternate in responding to which symbol was liked or not liked by others.

The present investigation has several notable strengths. First, the task was adapted from that of Mason and colleagues (2009) for use with a larger, mixed-gender, non-White sample. This approach helped uncover the basic mechanisms of neural processing of peer influence generalized to a broader segment of the population. Establishing the neural correlates engaged with this task can facilitate questions designed to address the mechanisms of social influence in different outcomes for adolescents and young adults such as consumerist behavior, social media use, and prosocial and deviant behavior. Second, the current findings contribute to the social affective neuroscience literature, which has principally focused on direct forms of peer influence (e.g., viewing stimuli alongside explicit peer ratings) to include more indirect forms of peer influence. Thus, these results speak to how young adults respond to subtle, incidental exposures to social cues of peer influence that mimic those pervasive in their everyday social environments (e.g., brand name logos). Future work should test if these findings hold for even subtler deliveries of group-level preferences (e.g., chart ratings of popular music). Third, this research benefited from using abstract symbols that held no social information prior to the study. Other work has used stimuli such as popular music (Berns et al., 2010) or facial attractiveness (Klucharev et al., 2009) to explore neural responses to peer preferences. Thus, using stimuli unfamiliar to the participant minimized the possibility of preference formation due to prior experience with the stimuli. Fourth, the simplicity of the task design is a notable strength. The findings demonstrated consistent and robust neural responses to abstract social information evaluated by others. This experimental design revealed an observable influence of even subtle, low-stakes social information on the brain. Nonetheless, future work is needed to determine the magnitude of these effects using more consequential peer information.

Limitations

Findings from the present study must be interpreted in the context of some limitations. First, socially tagged symbols were previously viewed by participants in repeated exposures outlined by a colored box preceding the fMRI scan, whereas novel symbols were not, a design feature that possibly influenced the saliency of these symbols. However, the results suggested that conscious familiarity did not drive these effects, based on data from a post-scan questionnaire that asked participants if they had viewed any of the symbols in the instantiation period. Additionally, the study findings speak only to information that has been rated by unknown peers rather than one's own friends. Much of the work in this area has relied on the perception of conforming to hypothetical peer groups (e.g., Gommans et al., 2017; Sherman et al., 2018), which may engage different neural circuitry than responding to information that has been rated by friends.

Conclusion

Taken together, exposure to implicit peer influence among young adults was found to engage brain regions that support salience detection and reward-processing, particularly when the influential information was unpopular. Although it will require further examination, it is possible that some individuals are more sensitive to what is disliked as opposed to liked by their peers. Further, we found that young adults who reported being more susceptible to peer influence displayed greater engagement of the insula and caudate to socially tagged information, although this was driven by a response to popular information. Additional work will be necessary to expand our understanding of individual differences in sensitivity to implicit peer influence. Focusing on the ways in which peer influence "gets into the brain" via subtle but reinforcing cues has the potential to identify those at risk for adverse effects of heightened sensitivity to peer influence, but also may be leveraged to promote positive outcomes. Moreover, in line with Schriber and Guyer (2016), the present study provided an initial characterization of the relation between neural response to implicit peer influence and an individual difference measure of peer sensitivity that may be relevant for future work on neurobiological susceptibility to social contexts.

Supplementary Material

Refer to Web version on PubMed Central for supplementary material.

Acknowledgments:

The authors thank Dr. Gang Chen for his helpful insight with data analysis.

Funding:

This research was supported by National Institute of Health grants R01MH098370 (AEG, PDH) and R01MH091068, a William T. Grant Foundation Scholars Award 180021 (AEG), a William T. Grant Mentoring Award 182606 (AEG), Prop. 63, the Mental Health Services Act and the Behavioral Health Center of Excellence at UC Davis (AEG), and a Jastro Shields Research Award (JSV).

References

Berns GS, Capra CM, Moore S, & Noussair C (2010). Neural mechanisms of the influence of popularity on adolescent ratings of music. NeuroImage, 49, 2687–2696. 10.1016/j.neuroimage.2009.10.070. [PubMed: 19879365]

Botvinik-Nezer R, Holzmeister F, Camerer CF, Dreber A, Huber J, Johannesson M, … & Avesani P (2020). Variability in the analysis of a single neuroimaging dataset by many teams. Nature, 1–7. 10.1038/s41586-020-2314-9

Brown B (1990). Peer groups. In: Feldman S; Elliott G, editors. At the threshold: The developing adolescent. Harvard University Press, 171–196.

Brown BB (2004). Adolescents' relationships with peers. Handbook of Adolescent Psychology, 2, 363–394. Hoboken, NJ: Wiley.

Chen G, Taylor PA, & Cox RW (2017). Is the statistic value all we should care about in neuroimaging? Neuroimage, 147, 952–959. 10.1016/j.neuroimage.2016.09.066 [PubMed: 27729277]

Choukas-Bradley S, Giletta M, Cohen GL, & Prinstein MJ (2015). Peer influence, peer status, and prosocial behavior: An experimental investigation of peer socialization of adolescents' intentions to volunteer. Journal of Youth and Adolescence, 44(12), 2197–2210. 10.1007/s10964-015-0373-2 [PubMed: 26525387]

Cox RW (1996). AFNI: Software for analysis and visualization of functional magnetic resonance neuroimages. Computers and Biomedical Research, 29, 162–173. [PubMed: 8812068]

Dahl R (2011). Understanding the risky business of adolescence. Neuron, 69, 837–839. 10.1016/j.neuron.2011.02.036 [PubMed: 21382545]

Eisenberger NI, Lieberman MD, & Williams KD (2003). Does rejection hurt? An fMRI study of social exclusion. Science, 302, 290–292. 10.1126/science.1089134 [PubMed: 14551436]

Elliott DS, Huizinga D, & Ageton SS (1985) Explaining delinquency and drug use. Beverly Hills, CA; Sage.

Fehse K, Simmank F, Gutyrchik E, & Sztrókay-Gaul A (2017). Organic or popular brands—food perception engages distinct functional pathways. An fMRI study. Cogent Psychology, 4, 1284392. 10.1080/23311908.2017.1284392

Gommans R, Sandstrom MJ, Stevens GW, ter Bogt TF, & Cillessen AH (2017). Popularity, likeability, and peer conformity: Four field experiments. Journal of Experimental Social Psychology, 73, 279–289. 10.1016/j.jesp.2017.10.001

Gibbons FX, Gerrard M, Lune LSV, Wills TA, Brody G, & Conger RD (2004). Context and cognitions: Environmental risk, social influence, and adolescent substance use. Personality and Social Psychology Bulletin, 30, 1048–61. 10.1177/0146167204264788 [PubMed: 15257788]

Guyer AE, Choate VR, Pine DS, & Nelson EE (2012). Neural circuitry underlying affective response to peer feedback in adolescence. Social Cognitive and Affective Neuroscience, 7, 81–92. 10.1093/scan/nsr043 [PubMed: 21828112]

Guyer AE, McClure-Tone EB, Shiffrin ND, Pine DS, & Nelson EE (2009). Probing the neural correlates of anticipated peer evaluation in adolescence. Child development, 80, 1000–1015. 10.1111/j.1467-8624.2009.01313.x [PubMed: 19630890]

Henrich J, Heine SJ, & Norenzayan A (2010). The weirdest people in the world? Behavioral and Brain Sciences, 33, 61–83.

Jarcho JM, Davis MM, Shechner T, Degnan KA, Henderson HA, Stoddard J, Fox NA, Leibenluft E, Pine DS, & Nelson EE (2016). Early-Childhood Social Reticence Predicts Brain Function in Preadolescent Youths During Distinct Forms of Peer Evaluation. Psychological Science, 27, 821–835. 10.1177/0956797616638319 [PubMed: 27150109]

Klucharev V, Hytönen K, Rijpkema M, Smidts A, & Fernández G (2009). Reinforcement learning signal predicts social conformity. Neuron, 61, 140–151. 10.1016/j.neuron.2008.11.027 [PubMed: 19146819]

Legare CH, & Harris PL (2016). The ontogeny of cultural learning. Child Development, 87, 633–642. 10.1111/cdev.12542 [PubMed: 27189392]

Li M, Xu H, & Lu S (2018). Neural basis of depression related to a dominant right hemisphere: A resting-state fMRI study. Behavioural neurology, 2018. 10.1155/2018/5024520

Mason MF, Dyer R, & Norton MI (2009). Neural mechanisms of social influence. Organizational Behavior and Human Decision Processes, 110, 152–159. 10.1016/j.obhdp.2009.04.001

McLean KC (2005). Late adolescent identity development: narrative meaning making and memory telling. Developmental Psychology, 41, 683. 10.1037/0012-1649.41.4.683 [PubMed: 16060814]

Mirman JH, & Curry AE (2016). Racing with friends: Resistance to peer influence, gist and specific risk beliefs. Accident Analysis & Prevention, 96, 180–184. 10.1016/j.aap.2016.08.014 [PubMed: 27543895]

Monahan KC, Steinberg L, & Cauffman E (2009). Affiliation with antisocial peers, susceptibility to peer influence, and antisocial behavior during the transition to adulthood. Developmental psychology, 45, 1520–1530. 10.1037/a0017417 [PubMed: 19899911]

Nelson EE, & Guyer AE (2011). The development of the ventral prefrontal cortex and social flexibility. Developmental cognitive neuroscience, 1, 233–245. 10.1016/j.dcn.2011.01.002 [PubMed: 21804907]

Nelson EE, Jarcho JM, & Guyer AE (2016). Social re-orientation and brain development: An expanded and updated view. Developmental Cognitive Neuroscience, 17, 118–127. 10.1016/j.dcn.2015.12.008 [PubMed: 26777136]

Psychology Software Tools, Inc. [E-Prime 2.0]. (2016). Retrieved from https://www.pstnet.com.

Sanfey AG, Rilling JK, Aronson JA, Nystrom LE, & Cohen JD (2003). The neural basis of economic decision-making in the ultimatum game. Science, 300, 1755–1758. doi:10.1126/science.1082976 [PubMed: 12805551]

Schriber RA, & Guyer AE (2016). Adolescent neurobiological susceptibility to social context. Developmental Cognitive Neuroscience, 19, 1–18. 10.1016/j.dcn.2015.12.009 [PubMed: 26773514]

Sherman LE, Greenfield PM, Hernandez LM, & Dapretto M (2018). Peer influence via Instagram: effects on brain and behavior in adolescence and young adulthood. Child Development, 89, 37–47. 10.1111/cdev.12838 [PubMed: 28612930]

Sherman LE, Payton AA, Hernandez LM, Greenfield PM, & Dapretto M (2016). The power of the like in adolescence: Effects of peer influence on neural and behavioral responses to social media. Psychological Science, 27, 1027–1035. 10.1177/0956797616645673 [PubMed: 27247125]

Spitzer M, Fischbacher U, Herrnberger B, Grön G, & Fehr E (2007). The neural signature of social norm compliance. Neuron, 56, 185–196. 10.1016/j.neuron.2007.09.011 [PubMed: 17920024]

Sanfey AG, Rilling JK, Aronson JA, Nystrom LE, & Cohen JD (2003). The neural basis of economic decision-making in the ultimatum game. Science, 300, 1755–1758. [PubMed: 12805551]

Shaffer D, Fisher P, Lucas CP, Dulcan MK, & Schwab-Stone ME (2000). NIMH Diagnostic Interview Schedule for Children Version IV (NIMH DISC-IV): description, differences from previous versions, and reliability of some common diagnoses. Journal of the American Academy of Child & Adolescent Psychiatry, 39(1), 28–38. 10.1097/00004583-200001000-00014 [PubMed: 10638065]

Somerville LH, Heatherton TF, & Kelley WM (2006). Anterior cingulate cortex responds differentially to expectancy violation and social rejection. Nature Neuroscience, 9, 1007–1008. 10.1038/nn1728 [PubMed: 16819523]

Stallen M, & Sanfey AG (2015). The neuroscience of social conformity: Implications for fundamental and applied research. Frontiers in neuroscience, 9, 337. 10.3389/fnins.2015.00337 [PubMed: 26441509]

Steinberg L, & Monahan KC (2007). Age differences in resistance to peer influence. Developmental Psychology, 43, 1531. 10.1037/0012-1649.43.6.1531 [PubMed: 18020830]

Taylor KS, Seminowicz DA, & Davis KD (2009). Two systems of resting state connectivity between the insula and cingulate cortex. Human Brain Mapping, 30, 2731–2745. 10.1002/hbm.20705 [PubMed: 19072897]

Turner JC (1991). Social Influence. Thomson Brooks/Cole Publishing Co.

Uddin LQ, Nomi JS, Hébert-Seropian B, Ghaziri J, & Boucher O (2017). Structure and Function of the Human Insula. Journal of Clinical Neurophysiology: Official Publication of the American Electroencephalographic Society, 34, 300–306. 10.1097/WNP.0000000000000377 [PubMed: 28644199]

Van Hoorn J, Van Dijk E, Güroğlu B, & Crone EA (2016a). Neural correlates of prosocial peer influence on public goods game donations during adolescence. Social Cognitive and Affective Neuroscience, 11, 923–933. 10.1093/scan/nsw013 [PubMed: 26865424]

van Hoorn J, van Dijk E, Meuwese R, Rieffe C, & Crone EA (2016b). Peer influence on prosocial behavior in adolescence. Journal of Research on Adolescence, 26(1), 90–100. 10.1111/jora.12173

Welborn BL, Lieberman MD, Goldenberg D, Fuligni AJ, Galván A, & Telzer EH (2016). Neural mechanisms of social influence in adolescence. Social Cognitive and Affective Neuroscience, 11, 100–109. 10.1093/scan/nsv095 [PubMed: 26203050]

Wentzel KR, & Muenks K (2016). Peer influence on students' motivation, academic achievement, and social behavior. Handbook of Social Influences in School Contexts: Social-emotional, Motivation, and Cognitive Outcomes, 13–30.

Xu Z, Zhang J, Wang D, Wang T, Zhang S, Ren X, … & Qu M (2019). Altered brain function in drug-naïve major depressive disorder patients with early-life maltreatment: a resting-state fMRI study. Frontiers in psychiatry, 10, 255. 10.3389/fpsyt.2019.00255 [PubMed: 31068844]

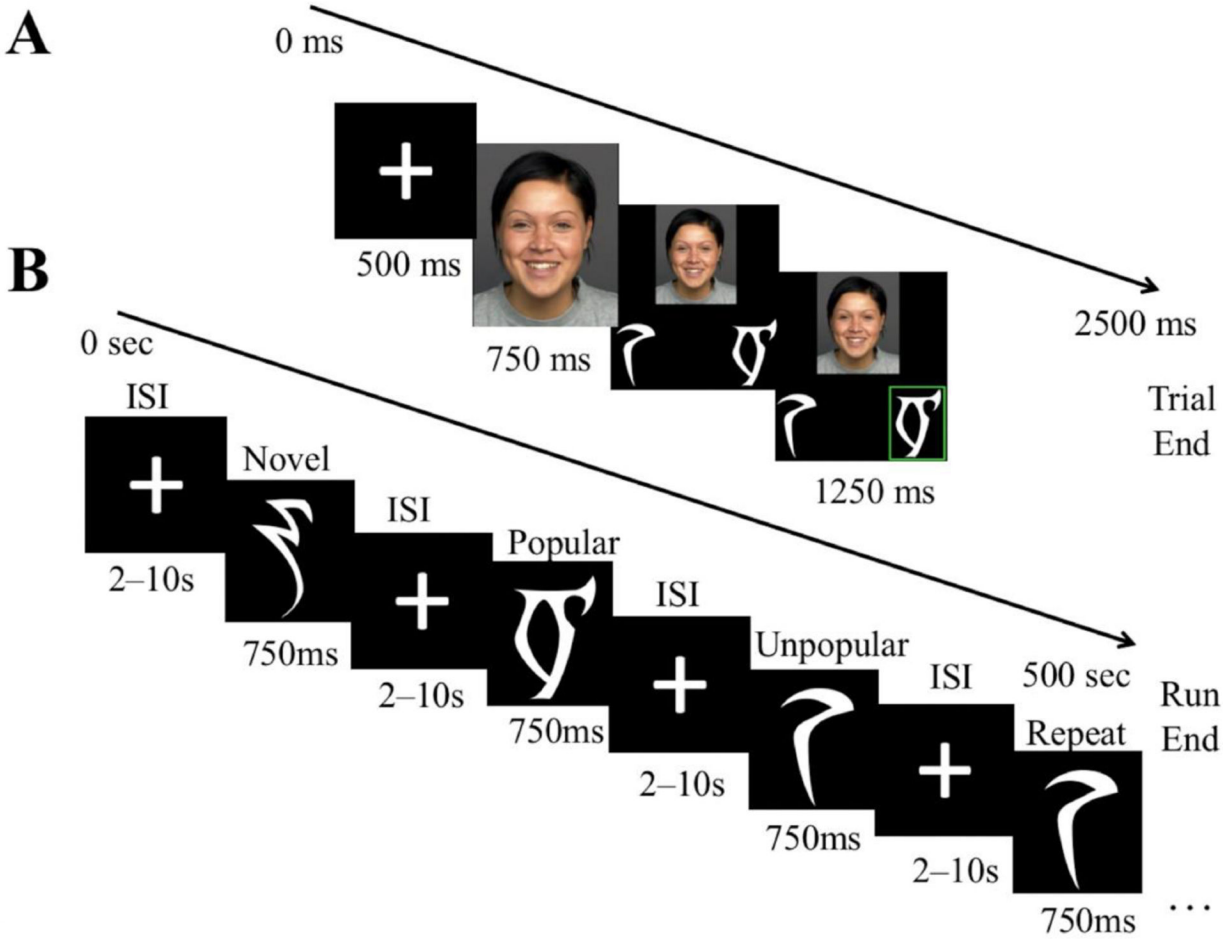

Figure 1.

(A) Timeline depicting one trial during the pre-scanning social "instantiation" phase. In each of the 200 trials, participants were presented with the face of a same-aged actor in the center of the screen for 750ms. Next, two symbols appeared below the face and a green box appeared around the target actor's preferred symbol, lasting 1250ms. Each trial was separated by a 500ms fixation cross. Participants were instructed to make a left or right button press to indicate which side of the screen the preferred symbol appeared. **(B)** Timeline depicting a sample run of the fMRI phase of the task. Symbols (popular, unpopular, and novel) were randomly presented one by one in the center of the screen, separated by 0–12s jittered inter-stimuli intervals (ISI) depicting fixation crosses to tease apart the signal associated with each symbol type. Participants were asked to press a button every time a symbol was presented twice in a row (representing a "repeat" trial).

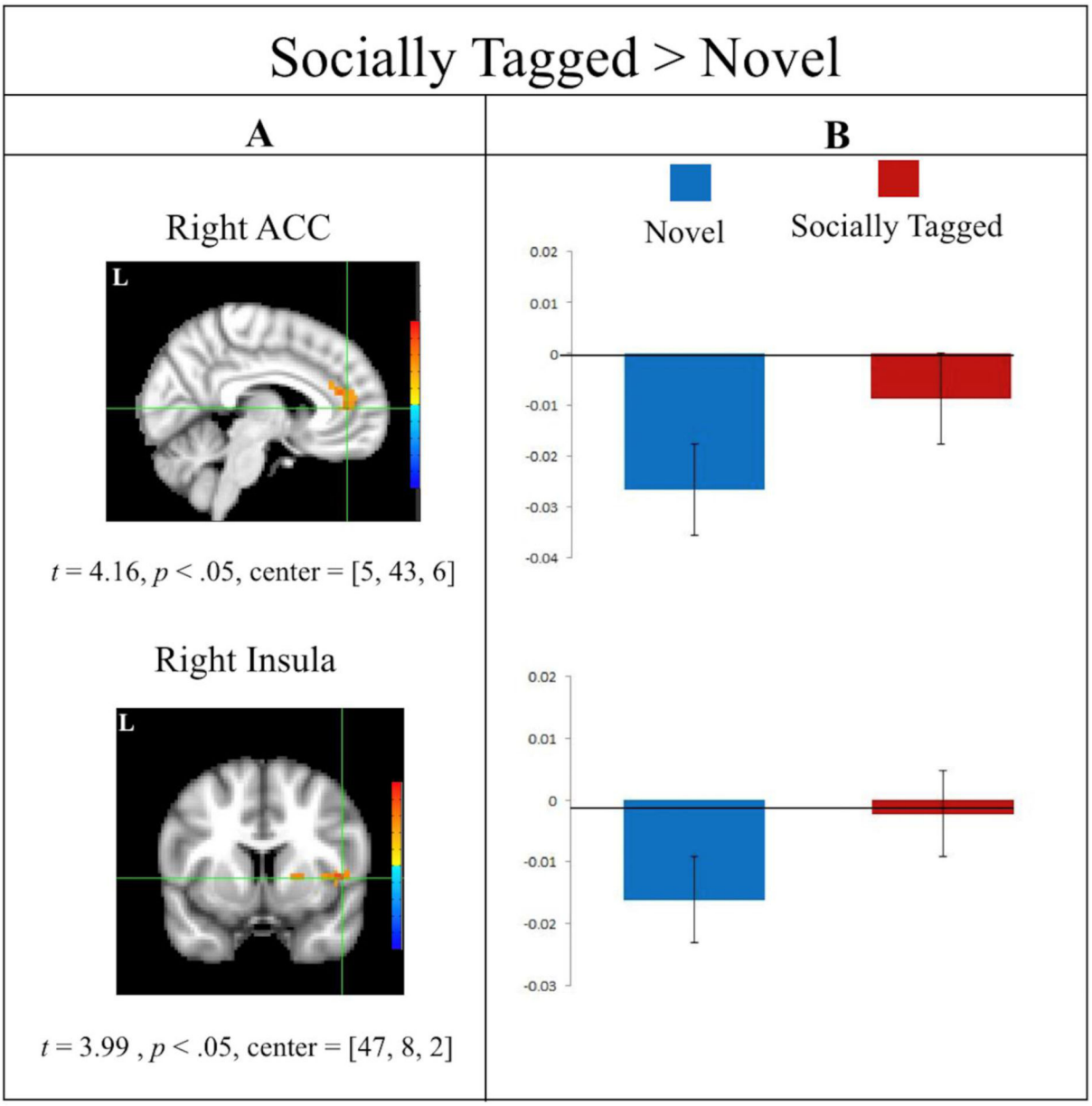

Figure 2.

(A) Significant clusters identified in whole-brain analysis. Images represent the direct comparison of socially tagged > novel symbols. Coordinates reflect the center of crosshairs for visualization. **(B)** Results of the region of interest analysis depicting standardized beta coefficients associated with the socially tagged (i.e., popular + unpopular) and novel symbols in each cluster. Values were computed by creating anatomical masks using AFNI atlases, extracting beta coefficients and averaging across all participants.

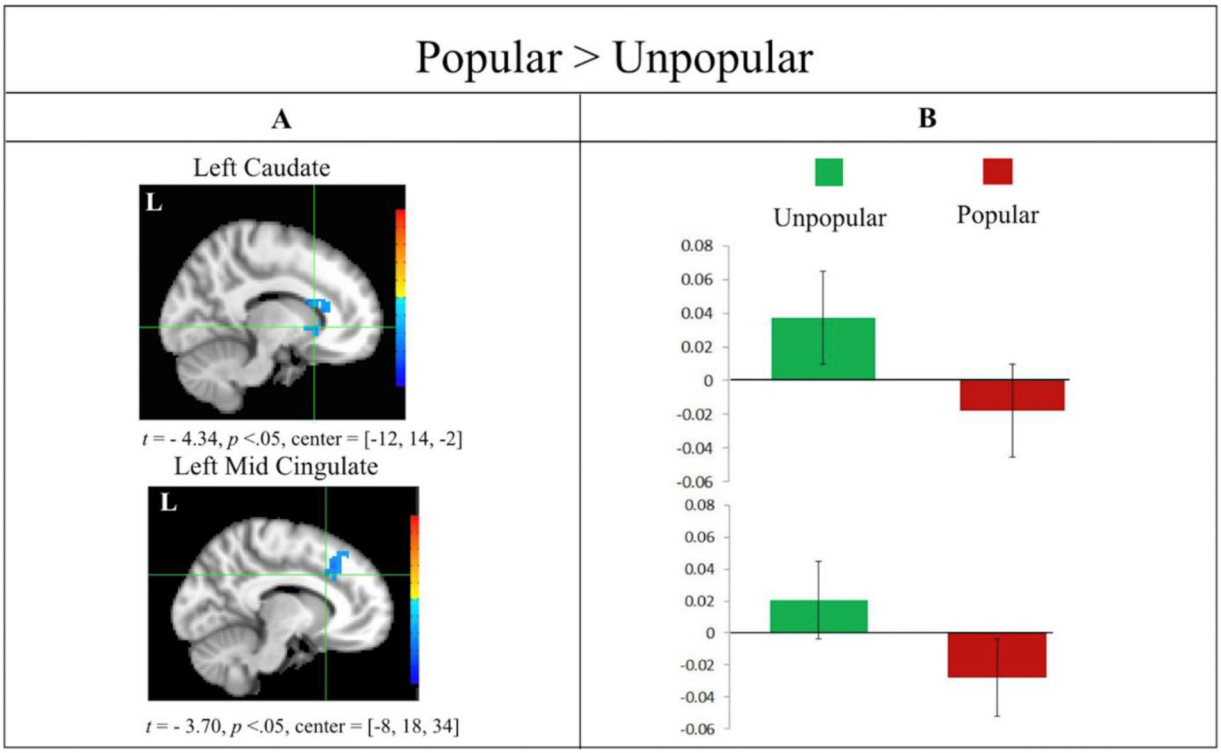

Figure 3.

(A) Significant clusters identified in whole-brain analysis. Images represent the direct comparison of popular > unpopular symbols. Coordinates reflect the center of crosshairs for visualization. **(B)** Results of the region of interest analysis depicting standardized beta coefficients associated with each symbol type (popular, unpopular) in each cluster. Values were computed by creating anatomical masks using AFNI atlases, extracting beta coefficients and averaging across all participants.

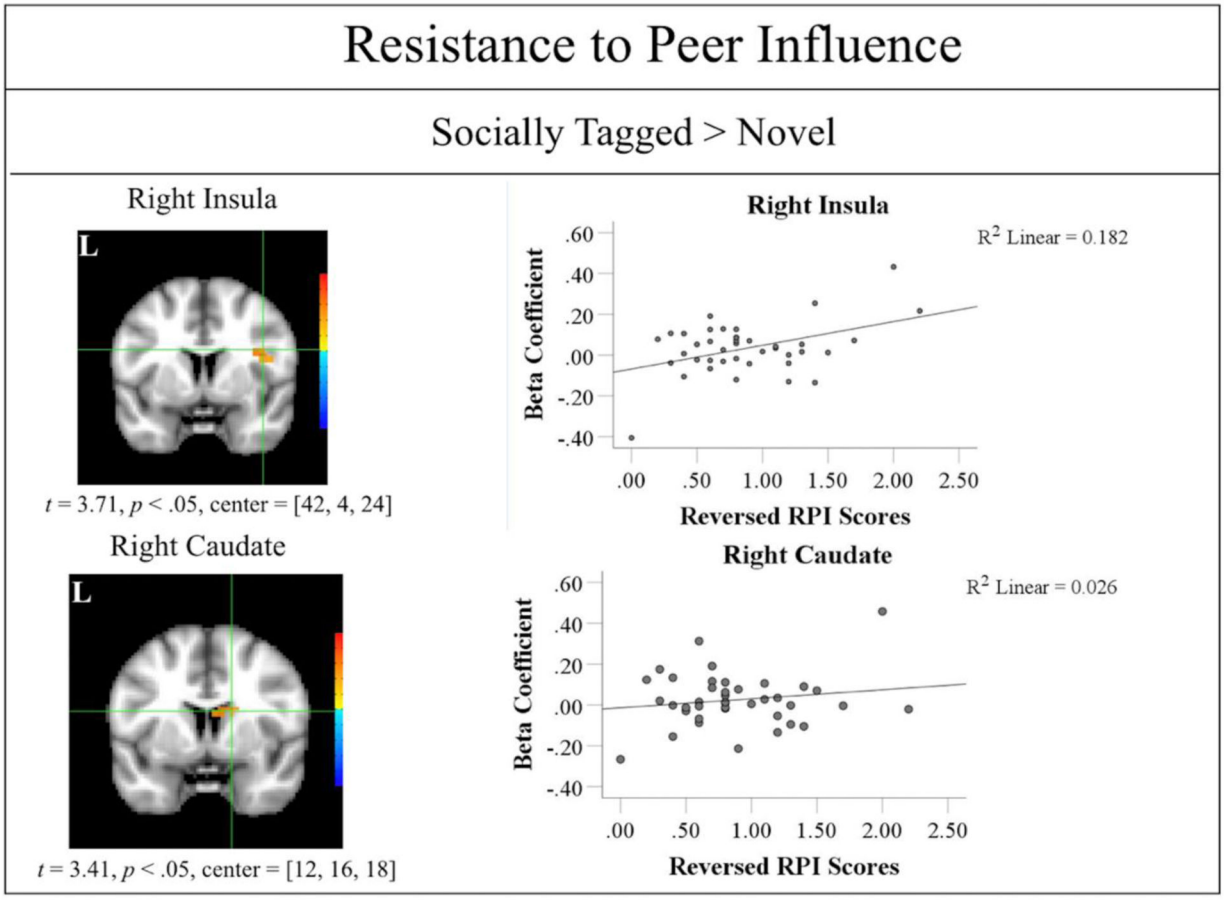

Figure 4.

Significant clusters identified in whole-brain analysis using the direct comparison of socially tagged > novel symbols. Coordinates reflect the center of crosshairs for visualization. Brain regions are accompanied with plots depicting participants' reversed scores on the Resistance to Peer Influence scale, with greater scores indicating more susceptibility, and beta coefficients of neural activation extracted from anatomical masks.

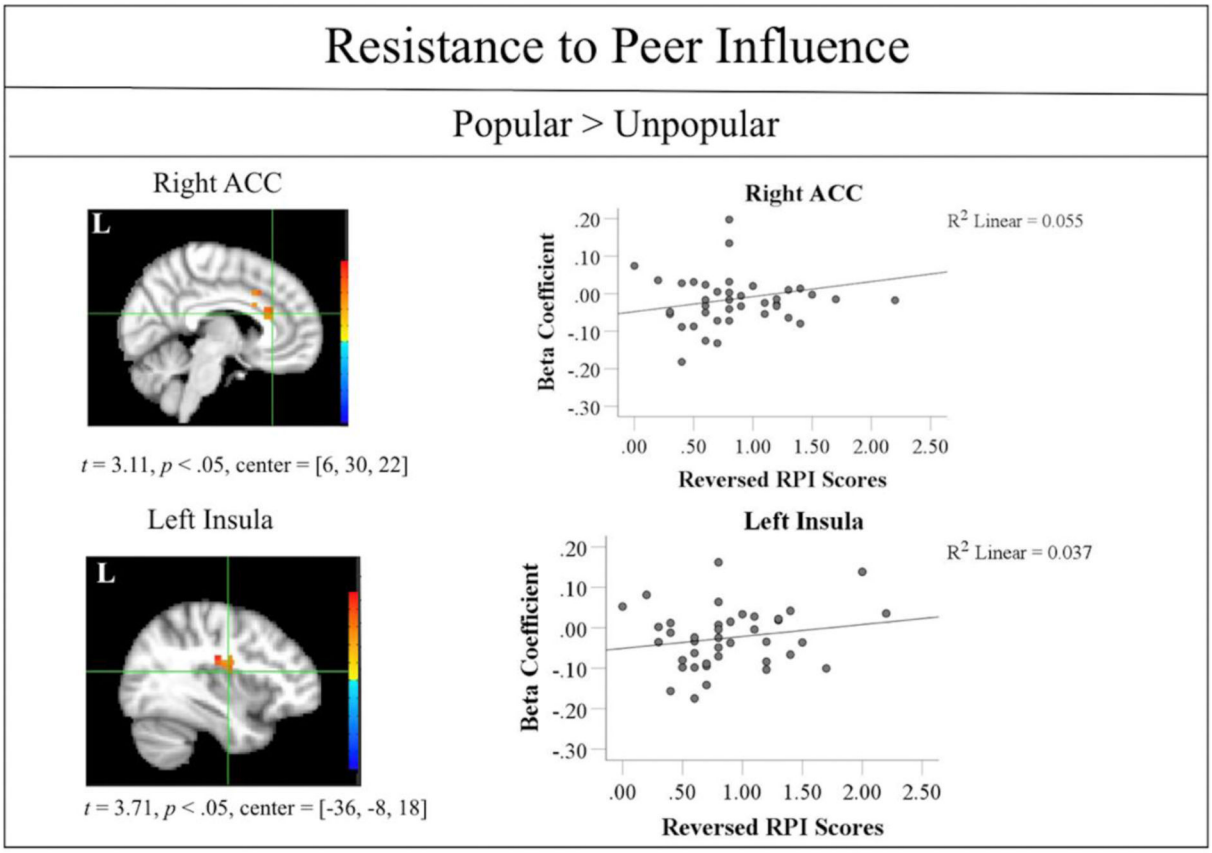

Figure 5.

Significant clusters identified in whole-brain analysis using the direct comparison of popular > unpopular symbols. Coordinates reflect the center of crosshairs for visualization. Brain regions are accompanied with plots depicting participants' reversed scores on the Resistance to Peer Influence scale and beta coefficients of neural activation extracted from anatomical masks.

Table 1.

Results from whole-brain analysis of clusters with differential activity when participants viewed socially tagged relative to novel symbols.

No. voxels	Peak (*x*, *y*, *z*)	t_{peak}	% signal change$_{peak}$	Region	G:W
285	58, 8, −26	4.19	.45	R. middle temporal	.74: .24
198	47, 12, 16	3.87	.17	R. inferior frontal	.50: .10
124	−23, −76, −12	4.12	.24	L. fusiform	.60: .30
103	47, 8, 2	3.99	.35	R. insula	.78: .18
81	−37, 1–3, 69	3.73	.16	L. precentral	.40: .10
50	5, 43, 6	4.16	.18	R. anterior cingulate	.87: .08
24	−30, −76, 41	2.70	.21	L. middle occipital	.62: .32
20	54, 5, 41	3.14	.15	R. precentral	.66: .29

Note: N= 43 (24 males, M_{Age} = 19.2 years). L. = Left; R. = Right. G:W = probability (*p*) of cluster occurring in gray vs. white matter, as identified by AFNI's *whereami* tool. Coordinates are reported in LPI MNI space. All identified clusters were significant at $p < .05$. Analysis included resistance to peer influence scores as covariate of interest and head motion, age 14 substance use recruitment status, and sex as nuisance variables. The anatomical region of each cluster identified was labeled using AFNI's *WhereAmI* function based on being the closest region within 3mm of the peak of activation around which the cluster was centered.

Table 2.

Results from whole-brain analysis of clusters with differential activity when participants viewed popular relative to unpopular symbols.

No. voxels	Peak (*x, y, z*)	t_{peak}	% signal change$_{peak}$	Region	G:W
483	48, 22, 41	−4.37	−.15	R. middle frontal	.73: .16
406	−47, −37, −5	−4.20	−.20	L. middle temporal	.90: .11
343	−23, 22, 20	−4.35	−.28	L. caudate	.81: .20
53	−12, 19, 34	−3.70	−.10	L. middle cingulate	.57: .38
49	30, −37, 16	−4.42	−.09	R. hippocampus	.58: .39
38	−68, −34, −5	−3.64	−.14	L. middle temporal	.71: .27
35	−51, −55, −22	−3.90	−.30	L. inferior temporal	.84: .14
32	−33, −72, 13	−4.21	−.07	L. middle occipital	.90: .12
23	54, −27, −8	−3.04	−.12	R. middle temporal	.84: .14
20	44, 29, −22	−3.33	−.42	R. inferior frontal	.40: .07

Note: N= 43 (24 males, M_{Age} = 19.2 years). L. = Left; R. = Right. G:W = probability (*p*) of cluster occurring in gray vs. white matter, as identified by AFNI's *whereami* tool. Coordinates are reported in LPI MNI space. All identified clusters were significant at $p < .05$. Analysis included resistance to peer influence scores as covariate of interest and head motion, age 14 substance use recruitment status, and sex as nuisance variables. The anatomical region of each cluster identified was labeled using AFNI's *WhereAmI* function based on being the closest region within 3mm of the peak of activation around which the cluster was centered.

Table 3.

Results from whole-brain analysis of clusters with differential activity based on resistance to peer influence scores when participants viewed socially tagged relative to novel symbols.

No. voxels	Peak (*x, y, z*)	t_{peak}	% signal change$_{peak}$	Region	G:W
400	65, −30, 13	3.88	.82	R. superior temporal	.65: .29
127	9, 37, 37	3.35	.33	R. superior medial	.57: .43
124	−54, −76, 2	3.50	.68	L. occipital	.47: .01
73	40, 5, 20	3.71	.24	R. insula	.86: .16
51	26, 40, 23	3.45	.28	R. middle frontal	.51: .49
46	12, 15, 20	3.41	.48	R. caudate	.86: .12
40	−30, −9, −33	3.17	1.63	L. fusiform	.72: .27
32	58, 19, 27	3.35	.36	R. inferior temporal	.67: .25
27	−65, −27, −8	3.29	.73	L. middle temporal	.75: .14
23	61, −23, −8	2.81	.17	R. middle temporal	.80: .15

Note: N= 43 (24 males, M_{Age} = 19.2 years). L. = Left; R. = Right. G:W = probability (*p*) of cluster occurring in gray vs. white matter, as identified by AFNI's *whereami* tool. Coordinates are reported in LPI MNI space. All identified clusters were significant at $p < .05$. Analysis included resistance to peer influence scores as covariate of interest and head motion, age 14 substance use recruitment status, and sex as nuisance variables. The anatomical region of each cluster identified was labeled using AFNI's *WhereAmI* function based on being the closest region within 3mm of the peak of activation around which the cluster was centered.

Table 4.

Results from whole-brain analysis of clusters with differential activity based on resistance to peer influence scores when participants viewed popular relative to unpopular symbols.

No. voxels	Peak (*x*, *y*, *z*)	t_{peak}	% signal change$_{peak}$	Region	G:W
46	−37, −20, 27	−2.80	−.21	L. insula	.56: .24
44	5, 29, 23	−3.05	−.21	R. anterior cingulate	.84: .14
29	−51, −34, 30	−2.41	−.35	L. supramarginal	.80: .21
29	12, −51, 48	−3.36	−1.35	R. precuneus	.72: .29
26	−19, −37, 13	−4.13	−.18	L. hippocampus	.31: .20
22	−19, 1, 16	−2.83	−.56	L. putamen	.93: .09
20	−9, −83, −8	1.22	.35	L. lingual	.75: .06

Note: N= 43(24 males, M_{Age} = 19.2 years). L. = Left; R. = Right. G:W = probability (*p*) of cluster occurring in gray vs. white matter, as identified by AFNI's *whereami* tool. Coordinates are reported in LPI MNI space. All identified clusters were significant at $p < .05$. Analysis included resistance to peer influence scores as covariate of interest and head motion, age 14 substance use recruitment status, and sex as nuisance variables. The anatomical region of each cluster identified was labeled using AFNI's *WhereAmI* function based on being the closest region within 3mm of the peak of activation around which the cluster was centered.